Sensors and Materials, Vol. 36, No. 2 (2024) 579–585
MYU Tokyo

S & M 3547

Scintillation Properties of Tb_4O_7–Al_2O_3 Glasses

Yuma Takebuchi,[1*] Atsunobu Masuno,[2] Daiki Shiratori,[3]
Kensei Ichiba,[1] Akihiro Nishikawa,[1] Takumi Kato,[1]
Daisuke Nakauchi,[1] Noriaki Kawaguchi,[1] and Takayuki Yanagida[1]

[1]Division of Materials Science, Nara Institute of Science and Technology (NAIST), Ikoma, Nara 630-0192, Japan
[2]Graduate School of Engineering, Kyoto University, Nishikyo-ku, Kyoto 615-8510, Japan
[3]Department of Electrical Engineering, Tokyo University of Science,
Niijuku, Katsushika-ku, Tokyo 125-8585, Japan

(Received October 30, 2023; accepted January 12, 2024)

Keywords: scintillator, glass, containerless method, radiation measurement

Undoped and Ce-doped Tb_4O_7–Al_2O_3 glasses without glass network-former oxides were synthesized by the containerless method. The X-ray diffraction measurement indicated that the synthesized glass samples were amorphous. In diffuse transmission spectra, the undoped sample showed absorption due to Tb^{4+}, and the reduction of Tb^{4+} to Tb^{3+} was observed in Ce-doped samples. In X-ray-induced scintillation spectra, the Ce-doped samples showed luminescence due to the 4f-4f transitions of Tb^{3+}. This result indicated that $CeCl_3$ acted as a reducer and enhanced the luminescence due to Tb^{3+}. In addition, the Ce-doped samples suppressed the thermally stimulated luminescence glow peaks at the low-temperature region.

1. Introduction

A scintillator, a type of phosphor for ionizing radiation detection, has a function to convert high-energy ionizing radiation into ultraviolet–visible–near-infrared photons. When combined with a photodetector, scintillators are used in many fields such as nuclear medicine,(1) security,(2) and high-energy physics.(3) In general, scintillators require high light yield, high chemical stability, low afterglow level, short decay time, and high energy resolution. For X- or γ-ray detection, a large effective atomic number (Z_{eff}) is also required. Because there are no scintillators with all of the above requirements, many researchers are still studying novel scintillators.(4–14) Until now, single crystalline scintillators are mainly used owing to their optical quality. Glass scintillators also have high optical quality and several industrial advantages over crystalline scintillators, such as low production cost, upsizing, and workability. On the other hand, glass scintillators tend to show a lower light yield than crystalline scintillators. Even a Li-glass scintillator, the only commercially available glass scintillator, has a light yield of about 1/10 those of crystalline scintillators.(15) Moreover, glass materials with a chemical composition resulting in a large Z_{eff} have been difficult to form. Because conventional melting methods generally need network-former oxides such as SiO_2, P_2O_5, and B_2O_3, the Z_{eff} of glasses becomes

*Corresponding author: e-mail: takebuchi.yuma.ty1@ms.naist.jp
https://doi.org/10.18494/SAM4751

ISSN 0914-4935

small. Therefore, novel glass scintillators with high light yield and large Z_{eff} should be developed.

Actually, some rapid quenching methods have been used to synthesize glasses without a network former.[16,17] However, the obtained glasses have a flake-like form; they are inappropriate for practical use as well as for measurements of fundamental physical properties. The containerless method prevents heterogeneous nucleation from occurring on the container walls and promotes the deep undercooling of the melt. As a result, the containerless method has been used to synthesize some glasses in bulk form with low-glass-forming-ability materials such as the R_2O_3–Al_2O_3 (R = rare-earth or Y) binary system without network-former oxides.[18] In the case of crystals, the R_2O_3–Al_2O_3 binary system allows the use of $RAlO_3$ perovskite and $R_3Al_5O_{12}$ garnet. Since the crystals have shown good scintillation properties, the glasses using the R_2O_3–Al_2O_3 binary system are also expected to show good scintillation properties.[19,20]

In this study, we synthesized Ce-doped Tb_4O_7–Al_2O_3 glasses by the containerless method and evaluated their radiation-induced luminescence properties. The Tb_4O_7–Al_2O_3 glasses have a large Z_{eff} (>50) owing to Tb. This Z_{eff} value is much larger than that of a Li-glass scintillator (22.8) and comparable to those of conventional crystalline scintillators such as Tl-doped NaI (50.7) and Tl-doped CsI (54.0). In addition, the Ce-doped $Tb_3Al_5O_{12}$, one of the Tb_4O_7–Al_2O_3 crystals, has shown a high light yield of 57,000 ph/MeV.[21] Therefore, the Tb_4O_7–Al_2O_3 glass is one of the candidates for a novel glass scintillator with large Z_{eff} and high light yield.

2. Materials and Methods

Tb_4O_7 (4N) and Al_2O_3 (4N) were mixed homogeneously. As a dopant, $CeCl_3$ (4N) powder was chosen to obtain Ce^{3+}. After mixing, the powders were pressed into tablets and sintered at 1400 °C for 8 h in air. Then, the tablets were crushed and the fragments were obtained. The containerless method was used to fabricate the glasses using the fragments.[22] The fragments were melted using a CO_2 laser (λ = 10.6 μm) during floating by O_2 gas flow. The melt was cooled to room temperature by turning off the laser. Ten pieces were prepared for each composition. Some of the pieces were crushed into powder to conduct the X-ray diffraction (XRD) measurement. A diffractometer (Rigaku, MiniFlex600) was used for the XRD measurement. The glass transition temperature (T_g) was investigated using a TG-DTA system (Hitachi, STA7200). A spectrophotometer (Shimadzu, SolidSpec-3700) was used to obtain diffuse transmission spectra. An original setup was used to investigate X-ray-induced scintillation spectra.[23] The bias voltage and tube current of an X-ray generator (Spellman, XRB80N100/CB) were set to 80 kV and 1.2 mA, respectively. Thermally stimulated luminescence (TSL) glow curves were examined using a TSL reader (NanoGray Inc., TL-2000).[24] The heating rate was 1 °C/s and the heating range was 50–490 °C. Before the TSL measurement, MiniFlex 600 irradiated X-rays to the samples.

3. Results and Discussion

By the containerless method, the samples with four different Tb contents were prepared. The Tb/(Tb + Al) = 30, 32, 37.5, and 40 samples were labeled as 30Tb, 32Tb, 37.5Tb, and 40Tb, respectively. The Z_{eff} values of the samples were 54.6, 54.7, 55.9, and 56.4, respectively. The Ce concentration was fixed at 1%. A Ce-free Tb/(Tb + Al) = 37.5 sample, with the same Tb/Al ratio as that of $Tb_3Al_5O_{12}$, was also prepared as a reference and labeled as undoped. Figure 1 shows a photograph of the prepared glasses. Spherical samples of 2 mm diameter were obtained. From the photograph, the color of the undoped sample was observed to be black, which changed to yellow after Ce doping. The Ce-doped samples with low Tb content showed a visibly light color.

Figure 2 shows the results of the XRD measurement of the samples. All the samples showed a halo peak at around 30° and no sharp peaks due to some crystalline phases were detected. Therefore, the synthesized samples were amorphous. The T_g values obtained from the DTA curves for the undoped, 30Tb, 32Tb, 37.5Tb, and 40Tb samples were 867, 864, 858, 855, and 859 °C, respectively.

Figure 3 shows the diffuse transmission spectra of the samples. The undoped sample showed an absorption band at a wavelength shorter than 570 nm. Because the Tb_4O_7 raw powder has the one-to-one mixture of Tb^{3+} and Tb^{4+}, the origin of the absorption was considered to be Tb^{4+}.[25–27] In the Ce-doped samples, the absorption shifted toward the short-wavelength region. Moreover, the samples with low Tb content exhibited the absorption at a short wavelength. From the relationship of complementary colors, the change in absorption wavelength corresponded to the visual color shown in Fig. 1. The results implied the reduction of Tb^{4+} to Tb^{3+}. Compared with the undoped and 37.5Tb samples, the only difference in the synthesis was the presence of $CeCl_3$. During melting, therefore, Cl_2 gas derived from $CeCl_3$ might have acted as a reducer. The change in the absorption wavelength among the Ce-doped samples was due to the difference in

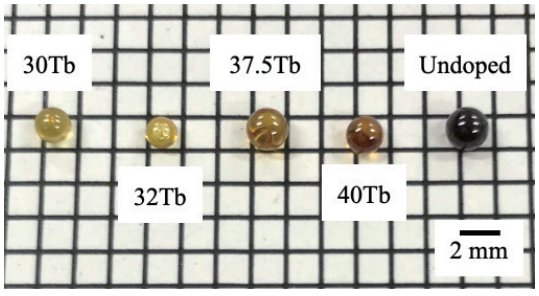

Fig. 1. (Color online) Photograph of synthesized samples.

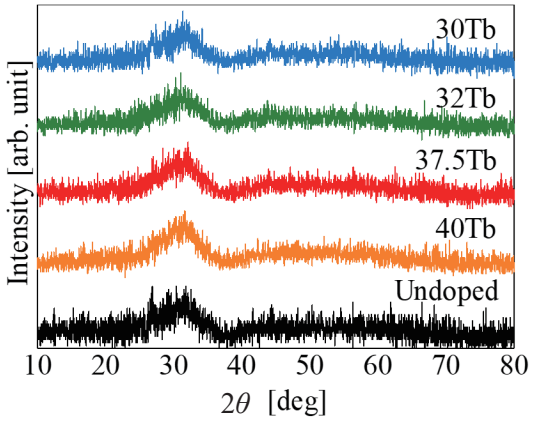

Fig. 2. (Color online) XRD patterns of samples.

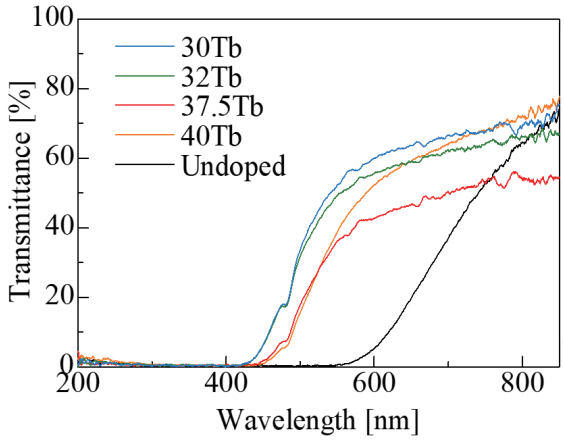

Fig. 3. (Color online) Diffuse transmission spectra of undoped and Ce-doped samples.

the amount of Tb^{4+}. The 4f–5d transitions of Ce^{3+} possibly contributed to the absorption at 400–500 nm.[21,28] A small absorption peak at 480 nm was also observed in the Ce-doped samples. The origin of the peak was the $^7F_6$–$^5D_4$ transitions of Tb^{3+}.[25]

Figure 4 shows the X-ray-induced scintillation spectra of the samples. Note that no valence changes such as the reduction of Tb^{4+} to Tb^{3+} or the oxidation of Tb^{3+} to Tb^{4+} induced by ionizing radiation were observed. In the undoped sample, no significant signals were detected. On the other hand, the Ce-doped samples showed an emission peak at 540 nm. Additionally, the samples with low Tb content also showed emission peaks at 490, 590, and 620 nm. From the emission wavelengths, the emission peaks at 490, 540, 590, and 620 nm were attributed to the 4f-4f transitions of Tb^{3+} ($^5D_4$–$^7F_6$, $^5D_4$–$^7F_5$, $^5D_4$–$^7F_4$, and $^5D_4$–$^7F_3$, respectively).[29–35] The relative emission intensity of the samples monitored at 540 nm is shown in Fig. 5. Corresponding to the result of diffuse transmittance, the samples doped with Ce had low Tb content and high luminescence intensity. One of the reasons for the difference in emission intensity was self-absorption. Although Ce^{3+} had no contribution to the luminescence, $CeCl_3$ decreased the amount of Tb^{4+} and increased the amount of Tb^{3+}. In this study, the samples were synthesized using Tb_4O_7 powder and O_2 gas; under this condition, Tb^{3+} oxidized easily to Tb^{4+}. The light yield of the glasses was unclear because of the low luminescence intensity, which might be caused by the presence of Tb^{4+}. The oxidation of Tb^{3+} to Tb^{4+} decreased the amount of the luminescence center and increased the effect of self-absorption. According to a previous study on the $TbAlO_3$ crystal, the crystal growth under a reducing (a mixture of nitrogen and hydrogen gases) atmosphere prevented the generation of Tb^{4+}, and the crystal showed strong Tb^{3+} luminescence.[25] Thus, the glass samples synthesized using a reducing gas flow are expected to show strong luminescence.

Figure 6 shows the TSL glow curves of the samples after X-ray irradiation of 100 Gy. The intensities were normalized at 400 °C. In the undoped sample, three glow peaks were observed at around 130, 200, and 400 °C, and the peak at 130 °C was dominant. In contrast, the peaks at

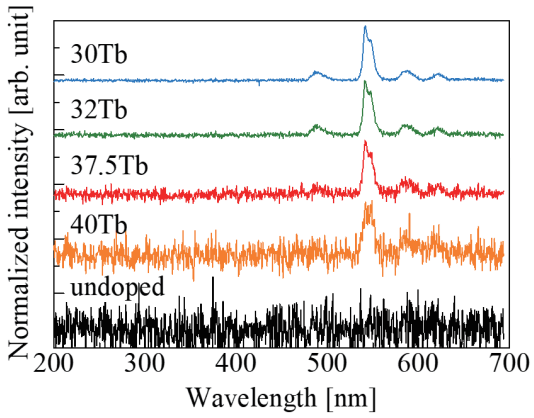

Fig. 4. (Color online) X-ray-induced scintillation spectra of samples.

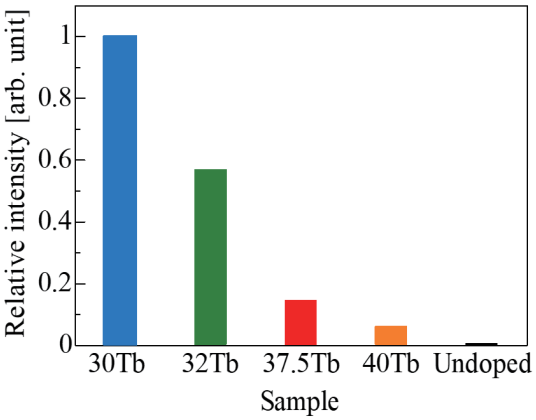

Fig. 5. (Color online) Comparison of luminescence intensity at 540 nm.

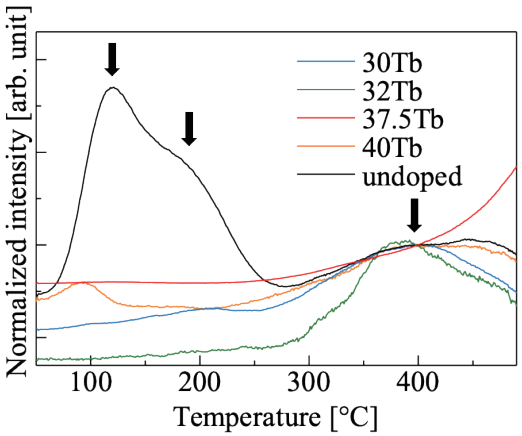

Fig. 6. (Color online) TSL glow curves of samples after X-ray irradiation of 100 Gy. The intensities were normalized at 400 °C.

130 and 200 °C were suppressed, and the peak at 400 °C was dominant in the Ce-doped samples. Note that the signal intensities included dark signals and that the signal at low temperature was predominantly a dark signal. In particular, the 37.5Tb sample indicated no significant signals, and only the signal due to black body radiation was observed. Although the luminescence origin in the TSL process was unclear, Tb^{3+} possibly acted as a luminescence center as with scintillation. The TSL glow peak means the presence of defects. Thus, the result indicated that the $CeCl_3$ doping into the glass suppressed the formation of defects in the undoped sample. The low temperature peaks are affected by room temperature and cause afterglow, although the measurement of the afterglow level of the present glasses was difficult because of the low signal intensity. Therefore, the Ce-doped samples are better than the undoped samples for scintillators from the viewpoint of afterglow.

4. Conclusions

Undoped and Ce-doped Tb_4O_7–Al_2O_3 glasses were fabricated by the containerless method. The glass samples without network-former oxides were successfully synthesized in bulk form. The Ce-doped samples showed luminescence due to the 4f–4f transitions of Tb^{3+}. Although Ce^{3+} has not affected the luminescence directly, doping $CeCl_3$ decreased the amount of Tb^{4+} and increased the amount of Tb^{3+}. As a result, the luminescence intensity increased owing to the reducing self-absorption. In addition, the Ce-doped samples suppressed the glow peaks at the low-temperature region and were expected to show low afterglow levels. In future work, investigating the effect of reducing gas flow during glass synthesis and other activators would be interesting to improve the scintillation properties.

Acknowledgments

This work was supported by Grants-in-Aid for Scientific Research A (22H00309), Scientific Research B (22H03872, 22H02939, 21H03733, and 21H03736), Early-Career Scientists (23K13689), Challenging Exploratory Research (22K18997), and JSPS Fellow (21J22668) from the Japan Society for the Promotion of Science. The Cooperative Research Project of the Research Center for Biomedical Engineering, Nippon Sheet Glass Foundation, Terumo Life Science Foundation, KRF Foundation, Tokuyama Science Foundation, Iketani Science and Technology Foundation, and Foundation for Nara Institute of Science and Technology are also acknowledged.

References

1 C. W. E. van Eijk: Nucl. Instrum. Methods Phys. Res., Sect. A **509** (2003) 17. https://doi.org/10.1016/S0168-9002(03)01542-0
2 J. Glodo, Y. Wang, R. Shawgo, C. Brecher, R. H. Hawrami, J. Tower, and K. S. Shah: Phys. Procedia **90** (2017) 285. https://doi.org/10.1016/j.phpro.2017.09.012
3 R. Mao, L. Zhang, and R.-Y. Zhu: IEEE Trans. Nucl. Sci. **55** (2008) 2425. https://doi.org/10.1109/TNS.2008.2000776
4 T. Yanagida, T. Kato, D. Nakauchi, and N. Kawaguchi: Jpn. J. Appl. Phys. **62** (2023) 010508. https://doi.org/10.35848/1347-4065/ac9026
5 M. Koshimizu: Jpn. J. Appl. Phys. **62** (2023) 010503. https://doi.org/10.35848/1347-4065/ac94fe
6 K. Okazaki, D. Nakauchi, H. Fukushima, T. Kato, N. Kawaguchi, and T. Yanagida: Sens. Mater. **35** (2023) 459. https://doi.org/10.18494/SAM4144
7 R. Nakamori, N. Kawano, A. Takaku, D. Onoda, Y. Takebuchi, H. Fukushima, T. Kato, K. Shinozaki, and T. Yanagida: Sens. Mater. **34** (2022) 707. https://doi.org/10.18494/SAM3689
8 Y. Takebuchi, D. Shiratori, T. Kato, D. Nakauchi, N. Kawaguchi, and T. Yanagida: Sens. Mater. **35** (2023) 507. https://doi.org/10.18494/SAM4142
9 Y. Takebuchi, M. Koshimizu, K. Ichiba, T. Kato, D. Nakauchi, N. Kawaguchi, and T. Yanagida: Materials **16** (2023) 4502. https://doi.org/10.3390/ma16134502
10 R. Nagaoka, N. Kawano, Y. Takebuchi, H. Fukushima, T. Kato, D. Nakauchi, and T. Yanagida: Jpn. J. Appl. Phys. **61** (2022) 110601. https://doi.org/10.35848/1347-4065/ac943d
11 T. Suto, N. Kawano, K. Okazaki, Y. Takebuchi, H. Fukushima, T. Kato, D. Nakauchi, and T. Yanagida: Jpn. J. Appl. Phys. **62** (2023) 010610. https://doi.org/10.35848/1347-4065/ac8f02
12 H. Kimura, T. Fujiwara, M. Tanaka, T. Kato, D. Nakauchi, N. Kawaguchi, and T. Yanagida: Sens. Mater. **35** (2023) 513. https://doi.org/10.18494/SAM4146

13 H. Fukushima, D. Nakauchi, T. Kato, N. Kawaguchi, and T. Yanagida: Sens. Mater. **35** (2023) 429. https://doi.org/10.18494/SAM4139
14 D. Shiratori, H. Fukushima, D. Nakauchi, T. Kato, N. Kawaguchi, and T. Yanagida: Sens. Mater. **35** (2023) 439. https://doi.org/10.18494/SAM4140
15 C. W. van Eijk, A. Bessière, and P. Dorenbos: Nucl. Instrum. Methods Phys. Res., Sect. A **529** (2004) 260. https://doi.org/10.1016/j.nima.2004.04.163
16 J. P. Coutures, G. Benezech, E. Antic-Fidancev, and M. Lemaitre-Blaise: Rev. Phys. Appl. **12** (1977) 667. https://doi.org/10.1051/rphysap:01977001205066700
17 S. Yajima, K. Okamura, and T. Shishido: Chem. Lett. **2** (1973) 1327. https://doi.org/10.1246/cl.1973.1327
18 Y. Watanabe, A. Masuno, and H. Inoue: J. Non-Cryst. Solids **358** (2012) 3563. https://doi.org/10.1016/j.jnoncrysol.2012.02.001
19 M. Koshimizu, Y. Fujimoto, and K. Asai: Sens. Mater. **35** (2023) 521. https://doi.org/10.18494/SAM4149
20 M. Akatsuka, D. Nakauchi, T. Kato, N. Kawaguchi, and T. Yanagida: Sens. Mater. **32** (2020) 1373. https://doi.org/10.18494/SAM.2020.2743
21 D. Nakauchi, G. Okada, N. Kawano, N. Kawaguchi, and T. Yanagida: Appl. Phys. Express **10** (2017) 072601. https://doi.org/10.7567/APEX.10.072601
22 A. Masuno: J. Ceram. Soc. Jpn. **130** (2022) 22073. https://doi.org/10.2109/jcersj2.22073
23 T. Yanagida, K. Kamada, Y. Fujimoto, H. Yagi, and T. Yanagitani: Opt. Mater. **35** (2013) 2480. https://doi.org/10.1016/j.optmat.2013.07.002
24 T. Yanagida, Y. Fujimoto, N. Kawaguchi, and S. Yanagida: J. Ceram. Soc. Jpn. **121** (2013) 988. https://doi.org/10.2109/jcersj2.121.988
25 M. Sekita, Y. Miyazawa, S. Morita, H. Sekiwa, and Y. Sato: Appl. Phys. Lett. **65** (1994) 2380. https://doi.org/10.1063/1.112682
26 D. F. Franco, Y. Ledemi, W. Correr, S. Morency, C. R. M. Afonso, S. H. Messaddeq, Y. Messaddeq, and M. Nalin: Sci. Rep. **11** (2021) 9906. https://doi.org/10.1038/s41598-021-89375-1
27 Z. Aoki, Y. Takebuchi, D. Nakauchi, T. Kato, N. Kawaguchi, and T. Yanagida: Opt. Mater. **134** (2022) 113068. https://doi.org/10.1016/j.optmat.2022.113068
28 Y. Onishi, T. Nakamura, and S. Adachi: Opt. Mater. **64** (2017) 557. https://doi.org/10.1016/j.optmat.2017.01.024
29 D. Nakauchi, H. Fukushima, T. Kato, N. Kawaguchi, and T. Yanagida: Sens. Mater. **34** (2022) 611. https://doi.org/10.18494/SAM3696
30 P. Kantuptim, T. Kato, D. Nakauchi, N. Kawaguchi, K. Watanabe, and T. Yanagida: Sens. Mater. **35** (2023) 451. https://doi.org/10.18494/SAM4141
31 K. Ichiba, Y. Takebuchi, H. Kimura, T. Kato, D. Nakauchi, N. Kawaguchi, and T. Yanagida: Sens. Mater. **35** (2023) 475. https://doi.org/10.18494/SAM4143
32 Y. Takebuchi, S. Honjo, K. Naoe, T. Kato, D. Nakauchi, N. Kawaguchi, and T. Yanagida: Crystals **12** (2022) 1620. https://doi.org/10.3390/cryst12111620
33 N. Kawaguchi, K. Watanabe, D. Shiratori, T. Kato, D. Nakauchi, and T. Yanagida: Sens. Mater. **35** (2023) 499. https://doi.org/10.18494/SAM4136
34 Y. Takebuchi, H. Fukushima, T. Kato, D. Nakauchi, N. Kawaguchi, and T. Yanagida: Jpn. J. Appl. Phys. **59** (2020) 052007. https://doi.org/10.35848/1347-4065/ab887c
35 Y. Takebuchi, M. Koshimizu, D. Shiratori, T. Kato, D. Nakauchi, N. Kawaguchi, and T. Yanagida: Radiat. Phys. Chem. **197** (2022) 110180. https://doi.org/10.1016/j.radphyschem.2022.110180